Supporting Information

Reconstituting intracellular vesicle fusion reactions – the essential role of macromolecular crowding

Haijia Yu[1#], Shailendra S. Rathore[1,2#], Chong Shen[1], Yinghui Liu[1], Yan Ouyang[1], Michael H. Stowell[1], and Jingshi Shen[1*]

[1]Department of Molecular, Cellular and Developmental Biology
University of Colorado at Boulder
Boulder, CO 80309, USA

[2]Present address: Applied and Engineering Physics
Cornell University
Ithaca, NY 14853

# These authors contributed equally to this work.

* Correspondence:
Phone: 303-492-6166; Fax: 303-492-7744
E-mail: jingshi.shen@colorado.edu

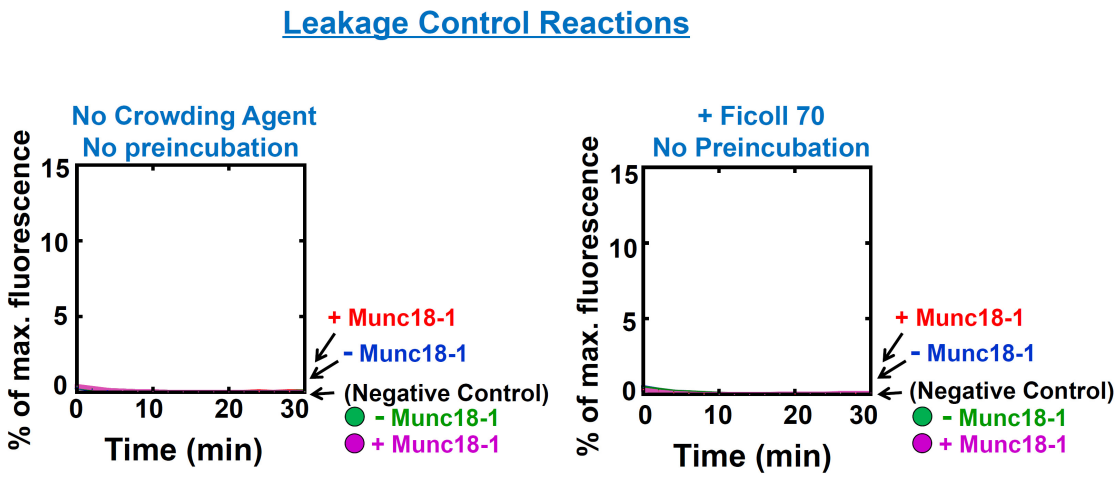

Figure S1. No content leakage was observed in Ficoll 70-containing fusion reactions mediated by SNAREs and Munc18-1. Liposome fusion reactions were performed in a similar way as in Fig. 1E except that the sulforhodamine B dye was included in both the v- and t-SNARE liposomes. The fusion reactions were performed in the absence or presence of 100 mg/ml Ficoll 70. Increases in sulforhodamine B fluorescence were not observed, indicating that no content leakage occurred during these fusion reactions.

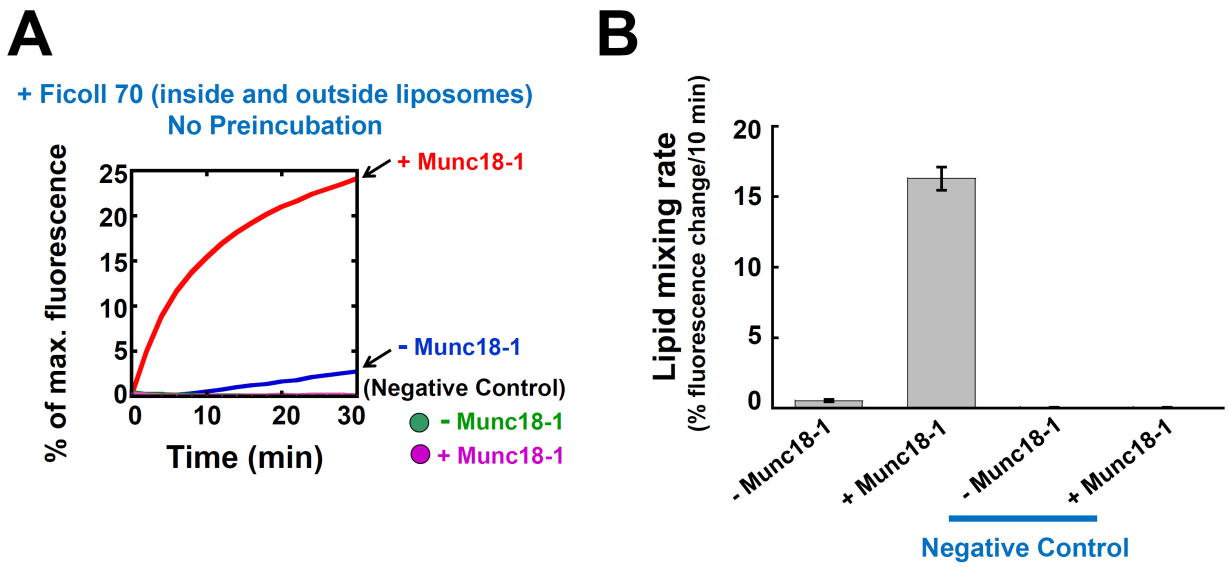

Figure S2. Reconstitution of Ficoll 70 into the lumen of proteoliposomes. (**A**) Liposome fusion reactions were performed in a similar way as in Fig. 1C except that 100 mg/ml Ficoll 70 was loaded into the v- and t-SNARE liposomes. The fusion reactions were performed in the presence of 100 mg/ml Ficoll 70. Inclusion of Ficoll 70 in the lumen of the liposomes eliminated the osmotic concentration gradient across liposome membranes. (**B**) Initial lipid-mixing rates of the fusion reactions shown in A. Error bars indicate standard deviation.

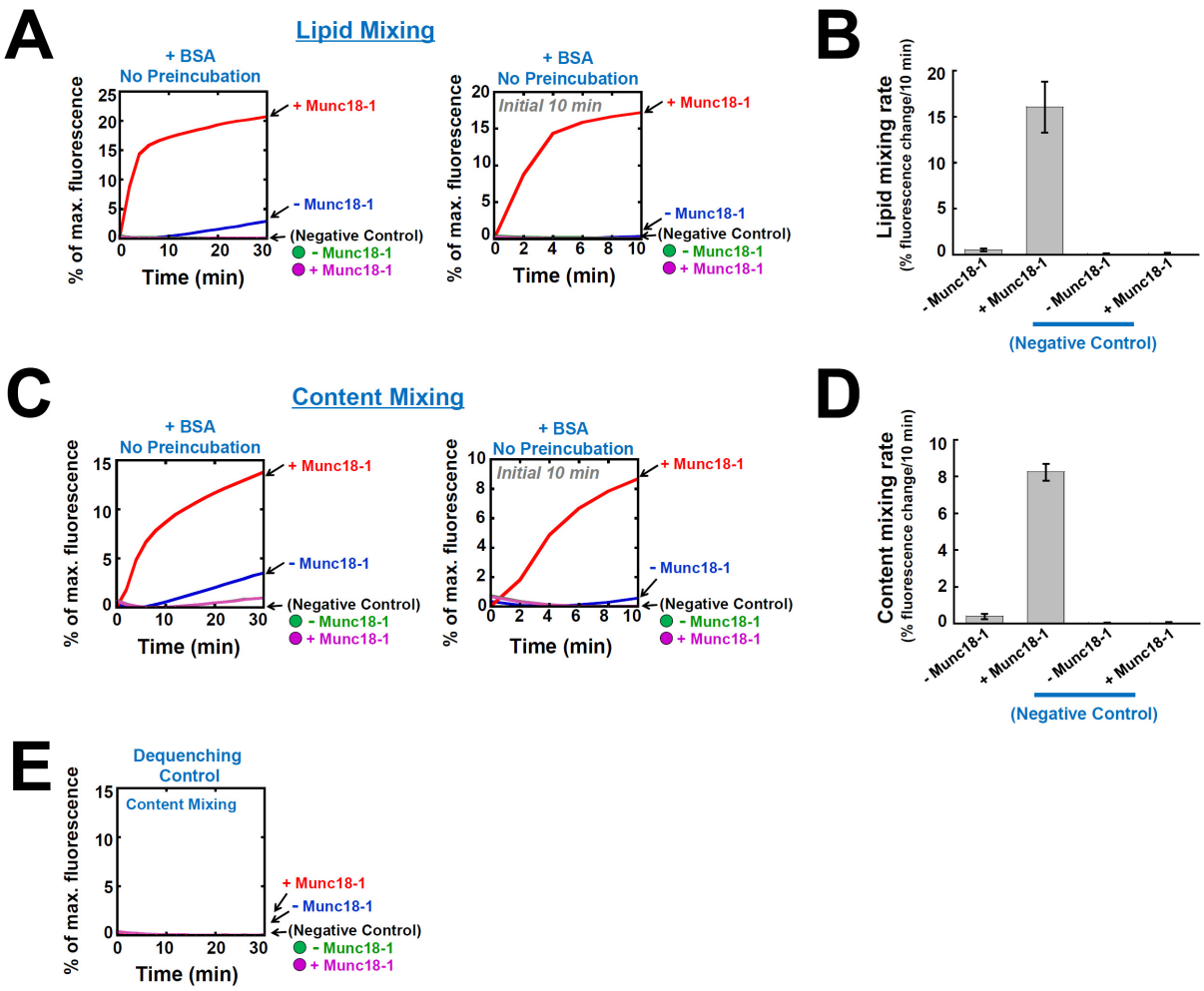

Figure S3. Munc18-1 promotes membrane fusion in the presence of the macromolecular crowding agent BSA. (**A**) Liposome fusion reactions were performed as described in Fig. 1C except that 100 mg/ml BSA was used in the place of Ficoll 70. The fusion reactions were measured using the FRET-based lipid mixing assay. The right graph depicts the first 10 minutes of the fusion reaction shown in the left graph, aiming to illustrate the stimulatory activity of Munc18-1 in the initial stage of the fusion reaction. (**B**) Initial lipid-mixing rates of the fusion reactions shown in A. Error bars indicate standard deviation. (**C**) Liposome fusion reactions were performed as described in Fig. 1E except that that 100 mg/ml BSA was used in the place of Ficoll 70. The fusion reactions were measured using the content mixing assay. The right graph depicts the first 10 minutes of the fusion reaction shown in the left graph. (**D**) Initial content-mixing rates of the fusion reactions shown in C. Error bars indicate standard deviation. (**E**) Leakage control reactions showing that no content leakage occurred in BSA-containing fusion reactions.

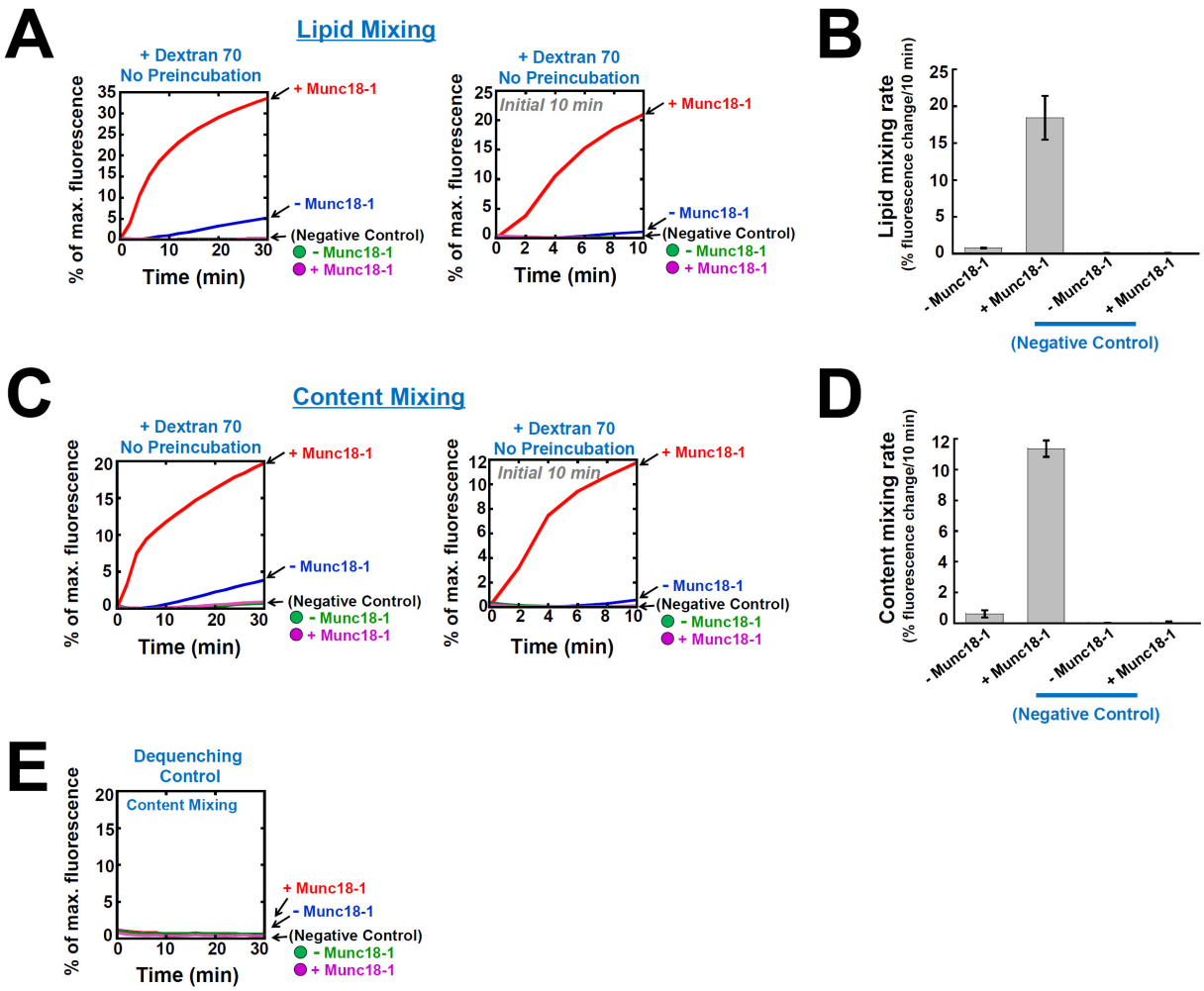

Figure S4. Munc18-1 promotes membrane fusion in the presence of the macromolecular crowding agent Dextran 70. (**A**) Liposome fusion reactions were performed as described in Fig. 1C except that 100 mg/ml Dextran 70 was used in the place of Ficoll 70. The fusion reactions were measured using the FRET-based lipid mixing assay. The right graph depicts the first 10 minutes of the fusion reaction shown in the left graph, aiming to illustrate the stimulatory activity of Munc18-1 in the initial stage of the fusion reaction. (**B**) Initial lipid-mixing rates of the fusion reactions shown in A. Error bars indicate standard deviation. (**C**) Liposome fusion reactions were performed as described in Fig. 1E except that that 100 mg/ml Dextran 70 was used in the place of Ficoll 70. The fusion reactions were measured using the content mixing assay. The right graph depicts the first 10 minutes of the fusion reaction shown in the left graph. (**D**) Initial content-mixing rates of the fusion reactions shown in C. Error bars indicate standard deviation. (**E**) Leakage control reactions showing that no content leakage occurred in Dextran 70-containing fusion reactions.

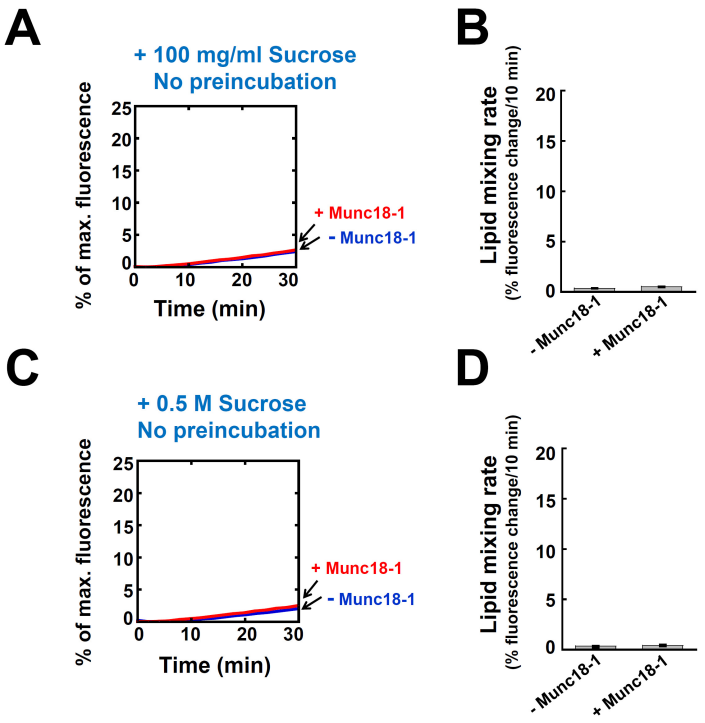

Figure S5. Munc18-1 does not promote membrane fusion in the presence of sucrose. (**A**) Liposome fusion reactions were performed as described in Fig. 1C except that 100 mg/ml sucrose was used in the place of Ficoll 70. The fusion reactions were measured using the FRET-based lipid mixing assay. (**B**) Initial lipid-mixing rates of the fusion reactions shown in A. Error bars indicate standard deviation. (**C**) Liposome fusion reactions were performed as described in Fig. 1C except that 0.5 M (171 mg/ml) sucrose was used in the place of Ficoll 70. The fusion reactions were measured using the FRET-based lipid mixing assay. (**D**) Initial lipid-mixing rates of the fusion reactions shown in C. Error bars indicate standard deviation.

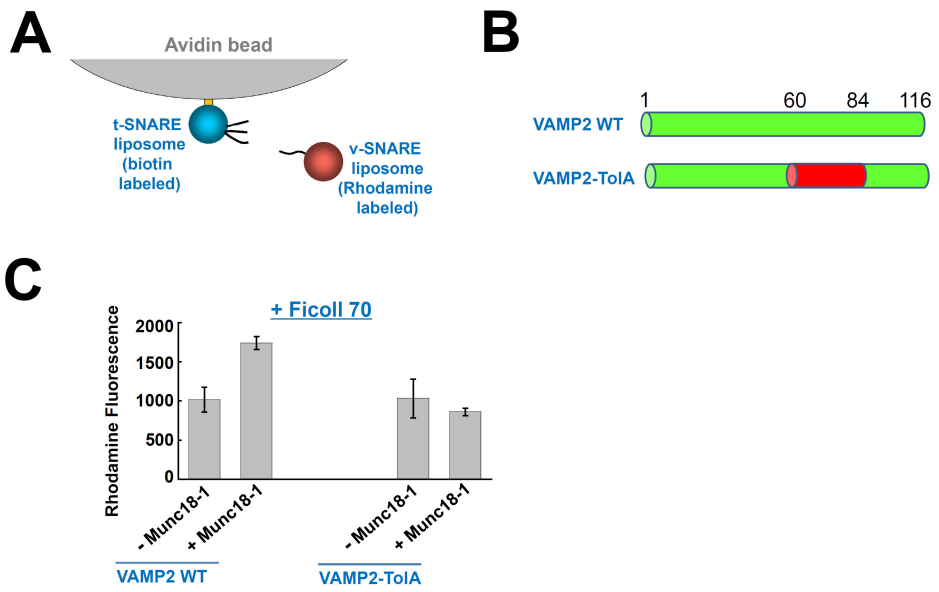

Figure S6. Munc18-1 primarily acts at the post-docking stage of the fusion reaction. (A) Diagram of the liposome pull-down assay [1,2]. **(B)** Diagrams of WT VAMP2 and the VAMP2-TolA chimera in which the a.a. 60-84 of VAMP2 was replaced with an unrelated sequence (*N*-GGSSIDAVMVDSGAVVEQYKRMQSQ-*C*) derived from the bacterial TolA protein. This VAMP2-TolA chimera can mediate liposome docking but not liposome fusion. (**C**) Measurements of the docking of t- and v-SNARE liposomes using the liposome pull-down assay. Biotin-labeled t-SNARE liposomes were anchored to avidin agarose beads and were used to pull down rhodamine-labeled v-SNARE liposomes. The binding reactions were performed at 4 °C for 1 hour in the absence or presence of 5 μM Munc18-1. All reactions were performed in the presence of 100 mg/ml Ficoll 70. Biotin-labeled protein-free liposomes were used as a negative control to obtain the background fluorescent signal. The background fluorescence was subtracted from other binding reactions to reflect specific SNARE-dependent liposome docking. The data are presented as rhodamine fluorescence intensity. Error bars indicate standard deviation.

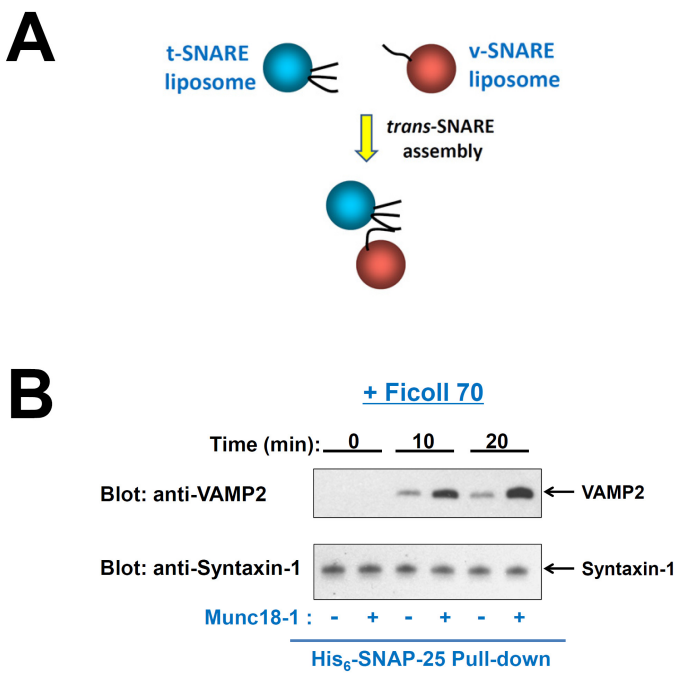

Figure S7. Munc18-1 promotes *trans*-SNARE zippering. (A) Diagram of the *trans*-SNARE formation assay [2,3]. **(B)** Reconstituted t- and v-SNARE liposomes were incubated at 4 °C for the indicated periods in the presence or absence of 5 μM Munc18-1 before 10-fold excess amount of inhibitory VAMP2 CD was added to block unpaired t-SNAREs. The liposomes were subsequently solubilized and the t-SNAREs were precipitated using nickel sepharose beads. Presence of FL VAMP2 in the precipitates was probed by western blotting, which was used as an indicator for *trans*-SNARE assembly between liposomes. All reactions were performed in the presence of 100 mg/ml Ficoll 70.

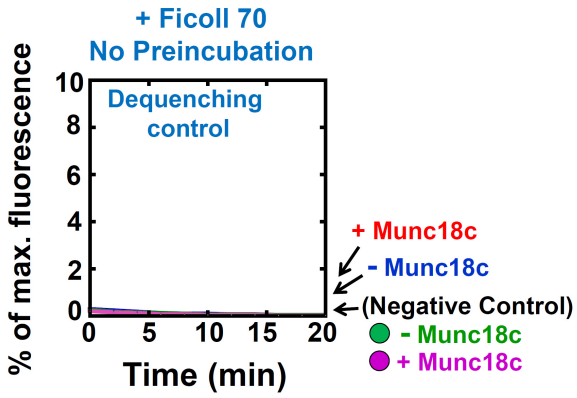

Figure S8. No content leakage occurred in crowding agent-containing fusion reactions mediated by SNAREs and Munc18c. Liposome fusion reactions were performed in a similar way as in Fig. 4C except that the sulforhodamine B dye was included in both the v- and t-SNARE liposomes. The fusion reactions were performed in the presence of 100 mg/ml Ficoll 70. Increases in sulforhodamine B fluorescence were not observed, indicating that no content leakage occurred during these fusion reactions.

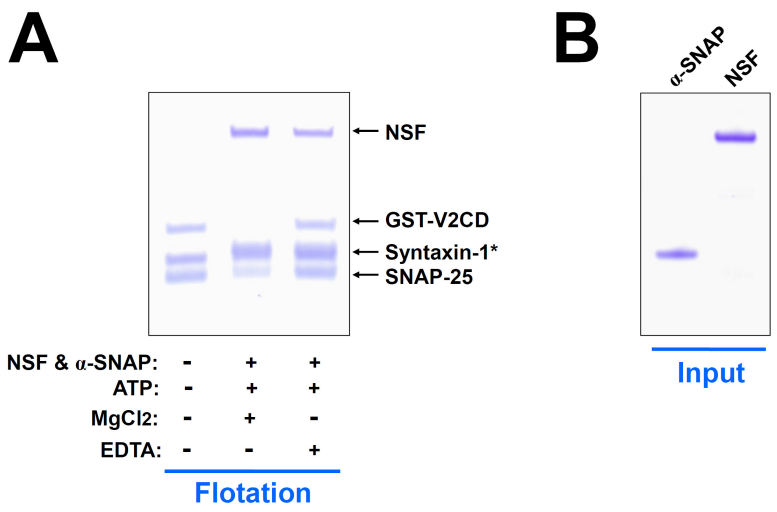

Figure S9. NSF and α-SNAP disassociate membrane-anchored *cis*-SNARE complexes. (A) Liposomes containing the t-SNARE complex (syntaxin-1 and SNAP-25) were incubated with the GST-tagged cytoplasmic domain of VAMP2 (GST-CDV2) for one hour at 4 ºC to assemble the *cis*-SNARE complex. Liposomes containing *cis*-SNARE complexes were incubated with NSF and α-SNAP (the Mg^{2+}-premix or EDTA-premix) at 37 ºC for one hour. After flotation on a Nycodenz gradient, proteins bound to the liposomes were resolved on SDS-PAGE and stained with coomassie blue. A fraction of SNAP-25 proteins were not released by NSF and α-SNAP because they faced the lumen of the liposomes. Asterisk: α-SNAP co-migrated with syntaxin-1 on SDS-PAGE. **(B)** Coomassie blue-stained SDS-PAGE gel showing the recombinant NSF and α-SNAP proteins used in this study.

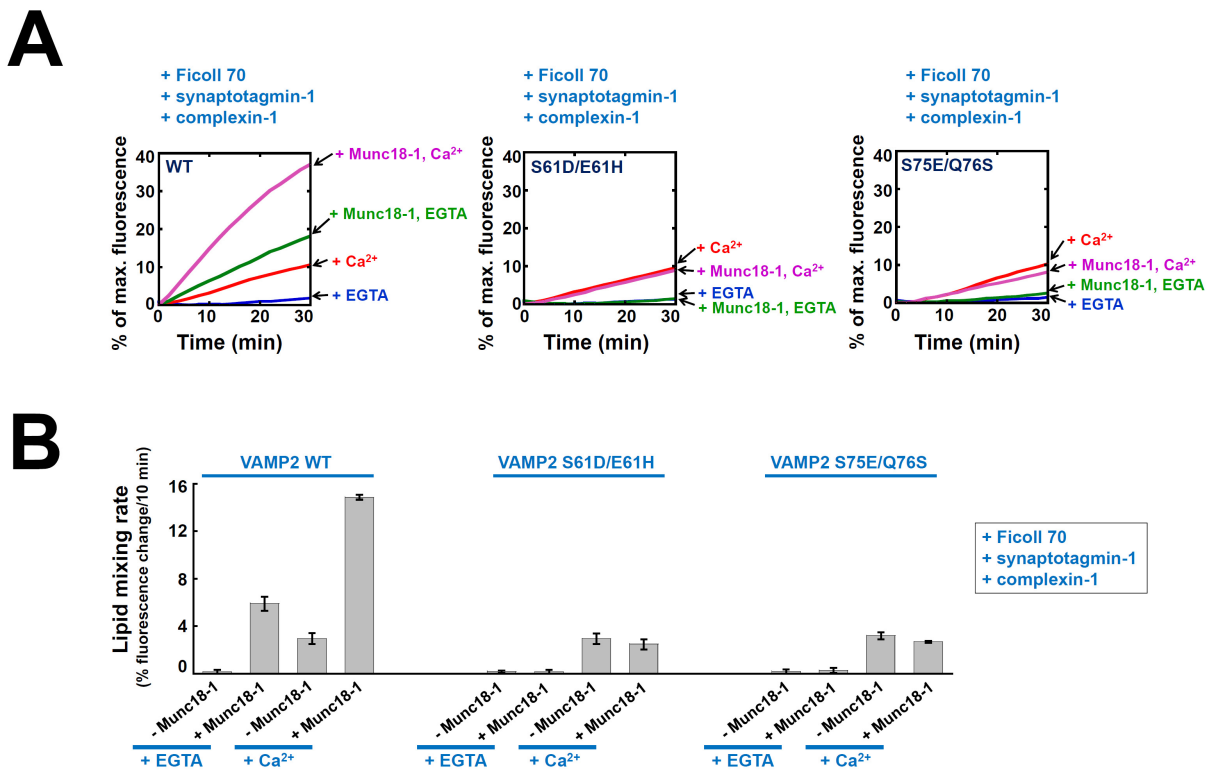

Figure S10. The stimulatory activities of Munc18-1 in the presence of synaptotagmin-1 and complexin-1. (A) The t-SNARE liposomes containing syntaxin-1 and SNAP-25 were reconstituted using the following lipid composition: 50% POPC, 20% POPE, 15% POPS, 10% cholesterol, 3% POPI, and 2% PIP2. The v-SNARE liposomes containing FL VAMP2 and synaptotagmin-1 were reconstituted using the following lipid composition: 47% POPC, 20% POPE, 15% POPS, 10% cholesterol, 5% POPI, 1.5% rhodamine-PE, and 1.5% NBD-PE. The v- and t-SNARE liposomes were mixed with 10 μM complexin-1 in the presence of 0.2 mM EGTA and 100 mg/ml Ficoll 70. The samples were incubated at 37 ºC for 20 min. Subsequently, 5 μM Munc18-1 (or equal volume of protein buffer) and 1 mM $CaCl_2$ (or 1 mM EGTA) were added and the fusion reactions were monitored for 30 min [4]. **(B)** Initial lipid-mixing rates of the fusion reactions shown in A (after Munc18-1/$CaCl_2$ addition). Error bars indicate standard deviation.

Supplementary Table 1

Effects of VAMP2 mutations on Munc18-1 activity *in vitro* and vesicle fusion *in vivo*

	VAMP2 Mutations	Munc18-1 Activity *in vitro*	Vesicle Fusion *in vivo*
WT	-	Normal	Normal [1-3]
M1	L32A/ T35A	Normal	Normal [1]
M2	V39A/ V42A	Normal	Normal [1]
M3	R56Q	Normal	Normal [2]
M4	L60A	Defective	Defective [3]
M5	L63A	Defective	Defective [3]
M6	L70A	Defective	Defective [1]
M7	F77A	Defective	Defective [1]

Sources of *in vivo* Data:

(1) Walter, A. M.; Wiederhold, K.; Bruns, D.; Fasshauer, D.; Sorensen, J. B. *J Cell Biol* **2010**, *188*, 401.

(2) Deak, F.; Shin, O. H.; Kavalali, E. T.; Sudhof, T. C. *J Neurosci* **2006**, *26*, 6668.

(3) This study.

Supplementary Table 2
Summary of Electrophysiological Data

Figure / Analyzed group	Analyzed parameter (unit) /Value (means±SEMs)	Number of cultures	Total number of neurons	*p* Value (Student's t-test)
Figure 6				
	mEPSC frequency (Hz)			
Control	2.98±0.37	4	18	control
VAMP2 KD	0.19±0.05	4	24	p<0.001
KD+VAMP2 WT	3.10±0.45	4	18	n.s.
KD+VAMP2 L63A	0.51±0.14	4	17	p<0.001
KD+VAMP2 L60A	0.88±0.13	4	24	p<0.001
	mEPSC amplitude (pA)			
Control	21.04±0.37	4	18	control
VAMP2 KD	19.57±0.40	4	24	n.s.
KD+VAMP2 WT	22.01±0.43	4	18	n.s.
KD+VAMP2 L63A	19.25±0.44	4	17	n.s.
KD+VAMP2 L60A	19.99±0.31	4	24	n.s.
	EPSC amplitude (pA)			
Control	384.86±48.61	3	20	control
VAMP2 KD	14.87±1.32	3	22	p<0.001
KD+VAMP2 WT	400.95±38.97	3	17	n.s.
KD+VAMP2 L63A	65.66±8.2	3	22	p<0.001
KD+VAMP2 L60A	79.06±9.4	3	13	p<0.001

n.s: not significant

Supplementary References

(1) Yu, H.; Rathore, S. S.; Shen, J. *J Biol Chem* **2013**, *288*, 18885.

(2) Yu, H.; Rathore, S. S.; Lopez, J. A.; Davis, E. M.; James, D. E.; Martin, J. L.; Shen, J. *Proc Natl Acad Sci U S A* **2013**, *110*, E3271.

(3) Shen, J.; Tareste, D. C.; Paumet, F.; Rothman, J. E.; Melia, T. J. *Cell* **2007**, *128*, 183.

(4) Wu, Y.; Gu, Y.; Morphew, M. K.; Yao, J.; Yeh, F. L.; Dong, M.; Chapman, E. R. *J Cell Biol* **2012**, *198*, 323.